Journal of Food Engineering 98 (2010) 248–256

Contents lists available at ScienceDirect

Journal of Food Engineering

journal homepage: www.elsevier.com/locate/jfoodeng

Residence time distribution in holding tubes using generalized convection model and numerical convolution for non-ideal tracer detection

Carola G.C.C. Gutierrez, Eduardo F.T.S. Dias, Jorge A.W. Gut *

Department of Chemical Engineering, Escola Politécnica, University of São Paulo, P.O. Box 61548, São Paulo, SP 05424-970, Brazil

ARTICLE INFO

Article history:
Received 19 October 2009
Received in revised form 16 December 2009
Accepted 3 January 2010
Available online 7 January 2010

Keywords:
Residence time distribution
Laminar flow model
Pasteurization
Aseptic processing

ABSTRACT

A procedure is proposed for the determination of the residence time distribution (RTD) of curved tubes taking into account the non-ideal detection of the tracer. The procedure was applied to two holding tubes used for milk pasteurization in laboratory scale. Experimental data was obtained using an ionic tracer. The signal distortion caused by the detection system was considerable because of the short residence time. Four RTD models, namely axial dispersion, extended tanks in series, generalized convection and PFR + CSTR association, were adjusted after convolution with the E-curve of the detection system. The generalized convection model provided the best fit because it could better represent the tail on the tracer concentration curve that is caused by the laminar velocity profile and the recirculation regions. Adjusted model parameters were well correlated with the flow rate.

1. Introduction

Many liquid food products, such dairy, fruit or egg products are subjected to continuous thermal processing for inactivation of undesired microorganisms and enzymes that compromise the food safety and shelf-life. Heat exchangers are used for rapidly heating and cooling the liquid stream, while a holding tube ensures the desired holding time at the processing temperature. The distributions of temperature and residence time in the holding tube are necessary to adequately evaluate the degree of thermal processing and to further minimize the deterioration of nutritional and sensorial characteristics caused by over-processing (Rao and Loncin, 1974a; Torres et al., 1998; Ibarrola et al., 2002; Gut et al., 2005).

Each element of fluid takes a different route and length of time to flow through a processing unit. The distribution of the these times at the unit outlet is called the E-curve or age distribution function, $E(t)$, which characterizes the residence time distribution (RTD) of the process. The simplest way to obtain the E-curve is by the pulse experiment, where a small amount of a non-reactive tracer is instantaneously injected at the unit inlet and its concentration is continuously recorded at the outlet, $C(t)$. The E-curve is then obtained from Eq. (1), where C_0 is the tracer background concentration and the area under the curve is unity, as in Eq. (2) (Levenspiel, 1999).

$$E(t) = \frac{C(t) - C_0}{\int_0^\infty C(t) - C_0 \, dt} \tag{1}$$

$$\int_0^\infty E(t)\, dt = 1 \tag{2}$$

The mean residence time is calculated from Eq. (3) and the dimensionless E-curve is obtained from Eq. (4), where $\theta = t/t_m$ is the dimensionless time.

$$t_m = \int_0^\infty t \cdot E(t)\, dt \tag{3}$$

$$E_\theta(\theta) = t_m \cdot E(t) \tag{4}$$

The analysis of the RTD data is very useful to study the flow pattern, to determine the degree of mixing and to diagnose flow problems such as recirculation, channeling, short-circuiting or stagnation. This technique is widely used for the evaluation of chemical reactors and packed beds (Levenspiel, 1989). In food processing, RTD analysis has been applied for assessing the effects of processing parameters on the flow characteristics of different process, particularly in aseptic processing (Torres and Oliveira, 1998a).

For tube flow, the RTD is associated with the velocity profile and the dispersion (turbulence). The ideal cases of parabolic velocity profile (laminar flow) and flat velocity profile (plug flow) rarely describe the flow in real systems. Since liquid foods often exhibit moderate viscosities, flow is usually laminar in the holding tube, which promotes a considerable dispersion on the residence time. The conservative approach is to use the minimum residence time, which occurs at the tube center at twice the mean velocity for Newtonian fluids, to determine the tube length. For a more rigorous approach, a RTD model that describes the flow pattern should

* Corresponding author. Tel.: +55 11 30912253; fax: +55 11 30912255.
E-mail address: jorgewgut@usp.br (J.A.W. Gut).

0260-8774/$ - see front matter © 2010 Elsevier Ltd. All rights reserved.
doi:10.1016/j.jfoodeng.2010.01.004

Nomenclature

a_i	model parameter (–)
c	electrical conductivity of solution (S/m)
C	concentration of tracer (kg/m^3)
C_0	background concentration of tracer (kg/m^3)
C_{in}	inlet concentration of tracer (kg/m^3)
C_{out}	outlet concentration of tracer (kg/m^3)
D_{ax}	axial dispersion coefficient (m^2/s)
D_{in}	internal diameter (m)
E	age distribution function, E-curve (s^{-1})
E_{DS}	E-curve of detection system (–)
E_{conv}	convoluted E-curve (–)
E_θ	dimensionless age distribution function (–)
L	tube length (m)
N	number of tanks in series (–)
m	number of experimental points (–)
Pe	Peclet number (–)
Q	volumetric flow rate (m^3/s)
R^2	coefficient of determination (–)
Re	Reynolds number (–)
SSE	sum of squared errors on E (s^{-2})
t, t'	time (s)
t_i, t_j	discrete time instants (s)
t_m	mean residence time (s)
t_{min}	minimum residence time (s)
T	temperature (K)
V	internal volume (m^3)
v	velocity (m/s)
V^A	active volume (m^3)
V^D	dead volume (m^3)
V^M	CSTR volume, mixed flow volume (m^3)
V^P	PFR volume, plug flow volume (m^3)

Greek letters

α	model parameter (–)
β	model parameter (–)
Γ	gamma function (–)
Δt	length of time step (s)
θ	dimensionless time (–)
θ_0	breakthrough time for laminar flow (–)
θ^P	breakthrough time for plug flow (–)
μ	viscosity (Pa s)
π	constant pi (π = 3.1416)
ρ	density (kg/m^3)
τ	spatial time (s)
τ^M	CSTR spatial time (s)
τ^P	PFR spatial time (s)

be taken into consideration for process design and product quality optimization.

The objectives of this work are to: (1) determine the RTD of two holding tubes used for milk pasteurization on laboratory scale; (2) present a generalized convection model to describe the laminar flow in curved tubes and adjust the model to the experimental data; (3) propose and use a mathematical procedure that takes into account the non-ideal detection of the tracer on the pulse experiment.

2. Residence time distribution models

Ideal flow models such as plug flow, perfectly mixed tank and laminar flow rarely reflect a real system with enough accuracy. Non-ideal models are usually derived from ideal models for accounting deviations implicit in real systems (Torres and Oliveira, 1998a). Models with one parameter, such as the well known dispersion model, are usually more adequate to represent tubular systems (Levenspiel and Bischoff, 1963). In this section, four single-parameter models are presented, which were used to fit the experimental RTD data of this work. The dimensionless E-curves of these models are illustrated in Fig. 1, where the effect of the model parameter can be observed.

2.1. Axial dispersion

The axial dispersion model is useful for representing small deviations from plug flow, as well as other non-ideal flow patterns in tubular systems. It has been widely applied to describe the flow in tubes and is the most frequent choice to model flow in holding tubes in aseptic processing (Torres et al., 1998). The model parameter is the Peclet number, which is defined for tube flow as $Pe = L \cdot v / D_{ax}$, where L is the tube length, v is the mean velocity and D_{ax} is the axial diffusion coefficient. This dimensionless number represents the relation between advection (flow) and diffusion. When Pe approaches infinity, negligible dispersion is observed (ideal plug flow). When Pe approaches zero, large dispersion is observed (perfectly mixed tank).

The axial dispersion model used in this work is the one presented by Gouvêa et al. (1990), as in Eq. (5). This equation is a simpler mathematical approximation of the analytical solution of the axial dispersion model with closed system boundary conditions.

$$E_\theta(\theta) = \sqrt{\frac{Pe+1}{4\cdot\pi\cdot\theta^3}}\exp\left(\frac{-(Pe+1)\cdot(1-\theta)^2}{4\cdot\theta}\right) \tag{5}$$

2.2. Extended tanks in series

The tanks in series model is based on a series of perfectly mixed tanks and can be used to represent deviations from plug flow and to represent real stirred tanks. The E_θ function for this model is presented in Eq. (6), where the parameter is the number of tanks, N.

$$E_\theta(\theta) = \frac{N\cdot(N\cdot\theta)^{N-1}}{(N-1)!}\exp(-N\cdot\theta) \tag{6}$$

In the "extended" tanks in series model, the number of tanks can assume non-integer values (Martin, 2000). To evaluate the factorial of a non-integer number in Eq. (6), the function Γ in Eqs. (7) and (8) is used.

$$\Gamma(N) = \int_0^\infty x^{N-1}\cdot e^{-x}\,dx \tag{7}$$

$$N! = \Gamma(N+1) = N\cdot\Gamma(N) = N\cdot(N-1)\cdot\Gamma(N-1) = \prod_{i=0}^{\mathrm{floor}(N-1)}(N-i)\cdot\Gamma[N-\mathrm{floor}(N-1)] \tag{8}$$

It can be observed in Fig. 1 that the dimensionless E-curve for the limiting case of $Pe = 0$ in the dispersion does not match the single perfectly mixed tank curve ($N = 1$) because of the mathematical approximation of Eq. (5).

2.3. Generalized convection model

For the convection model, the spread in RTD is attributed exclusively to the laminar velocity profile. Considering the parabolic

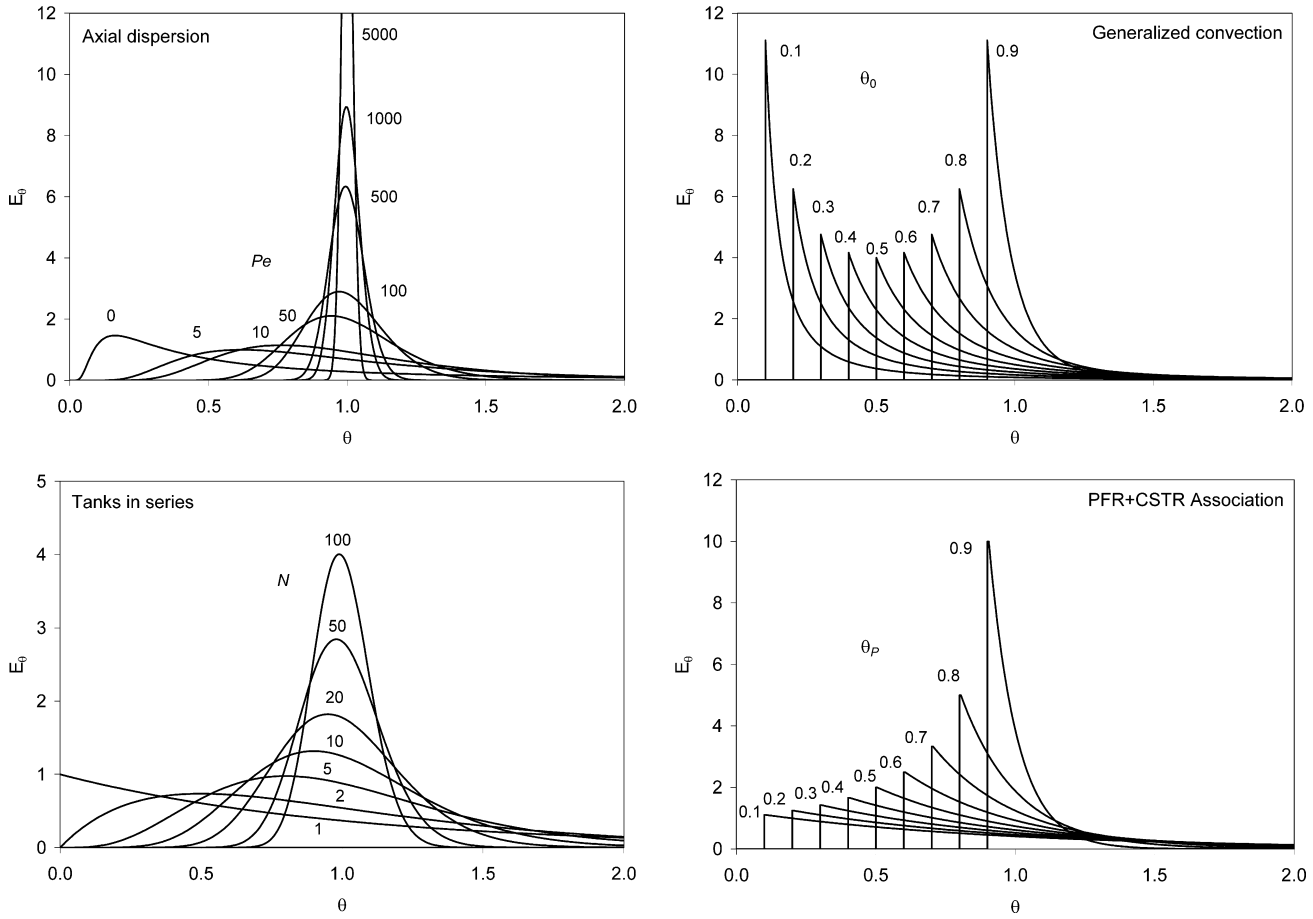

Fig. 1. Dimensionless E-curves for the RTD models considered in this work, showing effect of the model parameter. Curves obtained from Eqs. (5), (6), (12), and (13).

profile in tube flow, the pulse response (flux injection and detection) is given by the E and E_θ functions in Eqs. (9) and (10), which have no parameters. The mean residence time is the spatial time $\tau = Q/V$, where Q is the volumetric flow rate and V is the internal volume.

$$E(t) = \frac{\tau^2}{2}\frac{1}{t^3} \quad t \geqslant \frac{\tau}{2} \tag{9}$$

$$E_\theta(\theta) = \frac{1}{2}\frac{1}{\theta^3} \quad \theta \geqslant 0.5 \tag{10}$$

A generalized form of Eq. (10) can be derived using parameters α, β and θ_0 in Eq. (11). However, in order to satisfy Eqs. (2) and (3), the three parameters cannot be independent, which leads to the generalized convection model in Eq. (12) where the breakthrough time θ_0 is the only independent parameter (Levenspiel, 1989). Note that if $\theta_0 = 0.5$, Eq. (10) is obtained.

$$E_\theta(\theta) = \frac{\alpha \cdot \beta}{\theta^\beta} \quad \theta \geqslant \theta_0 \tag{11}$$

$$E_\theta(\theta) = \frac{1}{1-\theta_0}\frac{1}{\theta}\left(\frac{\theta_0}{\theta}\right)^{\frac{1}{1-\theta_0}} \quad \theta \geqslant \theta_0 \tag{12}$$

Analogous variations of the convection model were previously used by Ruthven (1971), Trivedi and Vasudeva (1974) and Nauman (1977) to describe laminar flow in helical coils and by Levien and Levenspiel (1999), Heibel et al. (2005) and Garcia-Serna et al. (2007) to describe flow in chemical reactors.

2.4. PFR + CSTR association

Compartment models or combined models are based on series and/or parallel associations of one or more ideal reactors, which are the plug flow reactor (PFR) and the continuously stirred tank reactor (CSTR). The volumes of the ideal reactors are adjusted so the E-curve of the association matches the experimental RTD data. Such models are very useful for diagnostic purposes and to detect faulty flow (Levenspiel and Bischoff, 1963; Levenspiel, 1999). Fillaudeau et al. (2009) successfully used a series association of one PFR and two CSTRs to represent the flow through a tubular Joule effect heater used for food heat treatment. In the present work, a series association of one PFR and one CSTR is considered. The PFR and CSTR volumes are V^P and V^M, respectively. The dead volume is obtained from $V^D = V - (V^P + V^M)$, where V is the internal volume of the real system (Himmelblau and Bischoff, 1968).

The spatial times of the ideal reactors are $\tau^P = V^P/Q$ and $\tau^M = V^M/Q$. Accordingly, the mean residence time of the system is $t_m = \tau^P + \tau^M$. The PFR + CSTR model can be written in terms of the breakthrough time of the plug flow reactor, $\theta^P = \tau^P/(\tau^P + \tau^M)$, as shown in Eq. (13).

$$E_\theta(\theta) = \frac{1}{1-\theta^P}\exp\left(\frac{\theta^P}{1-\theta^P} - \frac{\theta}{\theta^P}\right) \quad \theta \geqslant \theta^P \tag{13}$$

3. Correction for non-ideal tracer detection

The RTD data obtained from a pulse response experiment is affected by the way the tracer is injected and how it is detected (Hei-

bel et al., 2005). When measuring short residence times, as in holding tubes used for pasteurization and aseptic processing, the efficiency of the injection and detection systems are of considerable importance (Burton, 1958). The internal volume and shape of the injection and detection systems can distort the tracer signal, compromising the RTD results (Mills and Dudukovic, 1989). When it is not possible to produce an instantaneous pulse signal at the entrance of the process, a supplementary detection system has to be placed at the entrance of the process to record the input signal (Chakrabandhu and Singh, 2006; Fillaudeau et al., 2009).

Fig. 2 shows an example of non-ideal tracer detection. This type of signal distortion can occur when the internal volume of the detection system is not negligible compared to the internal volume of the process or when it promotes fluid recirculation.

It is possible to evaluate the non-ideality of the detection by injecting the tracer at the entrance of the detection system and determining its E-curve, which will differ by some degree from an ideal Dirac delta function. If the mean residence time is of the same order of magnitude of the mean residence time of the studied process, the signal distortion cannot be neglected. In this work, a mathematical procedure based on the convolution of signals is proposed to take into account this distortion when adjusting a RTD model in the time domain.

3.1. Convolution of signals

When a given one-shot input signal (C_{in}, concentration of the tracer versus time), passes through a vessel, it is modified into an output signal (C_{out}). This signal modification is related to the E-curve (input step response) of this vessel as in the convolution integral in Eq. (14). The convolution integral is a mathematical operation between two functions or signals to produce a third function that can be viewed as a cross-correlation product.

$$C_{out}(t) = \int_0^t C_{in}(t - t') \cdot E(t')\, dt' \tag{14}$$

When the input and output signals of a RTD experiment are known, it is possible to obtain the process E-curve from Eq. (14), where the convolution integral can be evaluated using Fourier or Laplace transforms. Alternatively, the convolution integral can be discretized in the time domain as in Eq. (15) (Levenspiel, 1999). In this equation, t_i and t_j represent discrete time instants and Δt is the length of the time step.

$$C_{out}(t_i) = \Delta t \cdot \sum_{j=1}^{i-1} C_{in}(t_{i-j}) \cdot E(t_j) \tag{15}$$

If the input signal C_{in} and the E-curve of the process are known, the discrete output signal can be obtained through Eq. (15), using the procedure presented in Table 1.

3.2. RTD model adjustment

The discrete convolution in Eq. (15) is used in this work in the following way: the RTD of the process, which is unknown, is considered to be the input signal to the detection system. Consequently, the recorded RTD data can be interpreted as the convolution of the RTD of the process with the E-curve of the detection system.

Fig. 3 shows the proposed procedure to obtain the RTD of the process, taking into account the signal distortion caused by the detection system. The experimental RTD data of the process and of the detection system must be obtained for the same conditions (fluid, flow rate and temperature). A proper model should be fitted to the detection system data in order to obtain the curve E_{DS}. A RTD model is chosen to represent the process behavior (E-curve) using initial estimates for the parameter and for the mean residence time. Finally, the convolution of signals E and E_{DS} should be fitted to the experimental data of the process by parameter estimation.

The estimation of the mean residence time along with the model parameter gives better results than calculating t_m from Eq. (7) before adjusting the dimensionless E-curve; especially for models with few parameters (Rangaiah and Krishnaswamy, 1990). In order to fit the E-curve model, its parameter and t_m are variables for the minimization of a given error function. The sum of squared errors in Eq. (16) can be used, for instance, where m is the number of experimental points. The summation terms can alternatively by multiplied by weight factors.

$$SSE = \sum_i^m (E_{\exp}(t_i) - E_{\text{conv}}(t_i))^2 \tag{16}$$

In this work, the convolution integral in Table 1 was constructed using software Excel (Microsoft, Redmond, USA) and the error function was minimized by varying both the model dimensionless parameter (Pe, N, θ_0 or θ_P) and the mean residence time of the process (t_m). The Solver feature of Excel, which uses a GRG2 algorithm, was applied to find the solution after a good estimate was first obtained by trial and error.

4. Experimental

4.1. Materials and methods

The RTD experiments were performed using the two holding tubes of a FT-43 laboratory plate pasteurizer (Armfield, Hampshire, UK). This unit for HTST pasteurization has a nominal capacity of 20 L/h, where the product is fed by a 7017-20 peristaltic pump (Masterflex, Vernon Hills, USA). Holding tubes T1 and T2 are shown in Fig. 4 and they can hold 75 and 200 mL, respectively. Tube T1 has a sinusoidal shape with three curves while tube T2 is helically

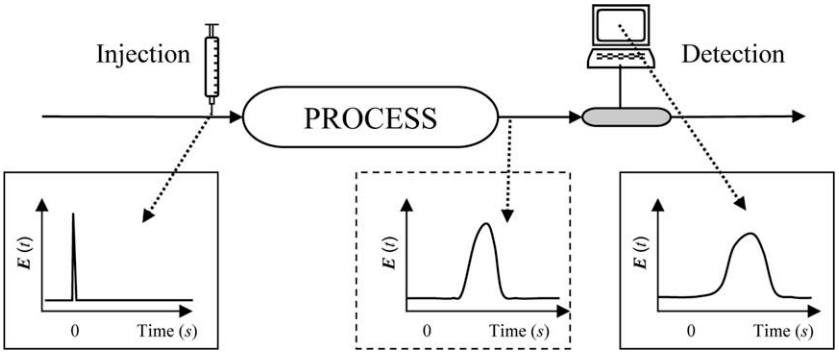

Fig. 2. Interference of tracer detection system on the RDT data.

Table 1
Numeric determination of the output signal using discrete convolution.

C_{out}	j = 1	j = 2	j = 3	j = 4	j = 5
$C_{out}(t_1)/\Delta t=$	0				
$C_{out}(t_2)/\Delta t=$	$C_{in}(t_1)\cdot E(t_1)+$	0			
$C_{out}(t_3)/\Delta t=$	$C_{in}(t_2)\cdot E(t_1)+$	$C_{in}(t_1)\cdot E(t_2)+$	0		
$C_{out}(t_4)/\Delta t=$	$C_{in}(t_3)\cdot E(t_1)+$	$C_{in}(t_2)\cdot E(t_2)+$	$C_{in}(t_1)\cdot E(t_3)+$	0	
$C_{out}(t_5)/\Delta t=$	$C_{in}(t_4)\cdot E(t_1)+$	$C_{in}(t_3)\cdot E(t_2)+$	$C_{in}(t_2)\cdot E(t_3)+$	$C_{in}(t_1)\cdot E(t_4)+$	0
$C_{out}(t_6)/\Delta t=$	$C_{in}(t_5)\cdot E(t_1)+$	$C_{in}(t_4)\cdot E(t_2)+$	$C_{in}(t_3)\cdot E(t_3)+$	...	...
$C_{out}(t_7)/\Delta t=$	$C_{in}(t_6)\cdot E(t_1)+$	$C_{in}(t_5)\cdot E(t_2)+$	...	...	...
$C_{out}(t_8)/\Delta t=$	$C_{in}(t_7)\cdot E(t_1)+$	...	...	...	...
...	...	...	...	...	...

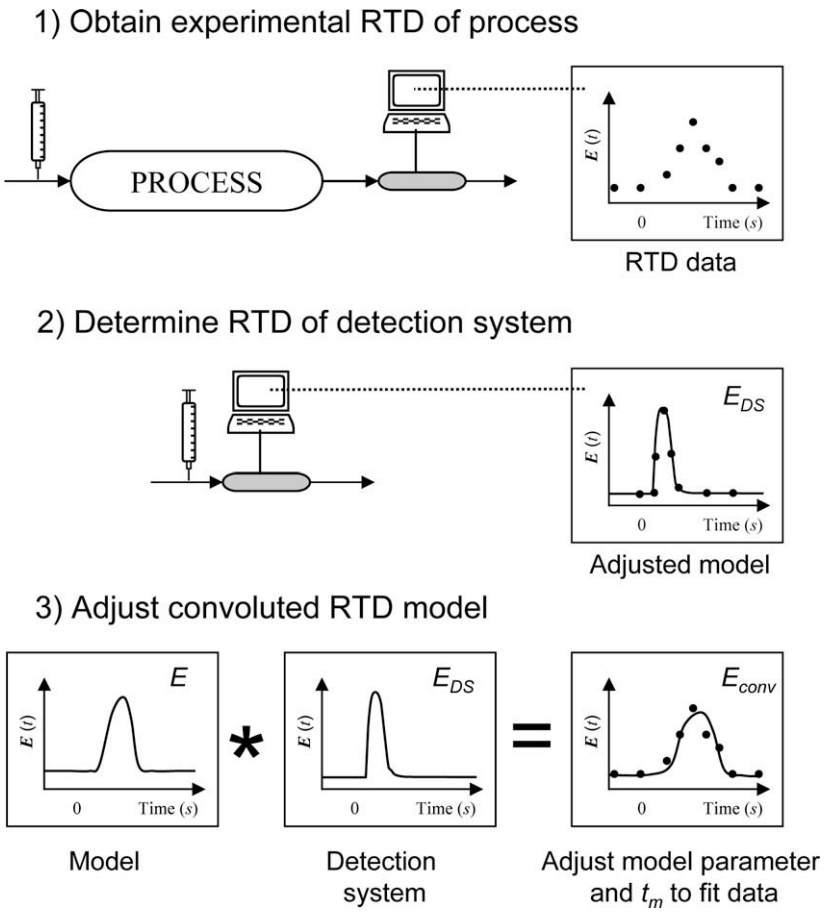

Fig. 3. Procedure to fit the RTD model to the experimental data, taking into account the signal distortion caused by the detection system.

Fig. 4. Holding tubes T1 and T2 of the FT-43 laboratory plate pasteurizer (thermal insulation of T2 was removed for better view).

coiled. External and internal diameters are 1.27 and 1.07 cm for T1 and 1.27 and 0.93 cm for T2.

4.2. Measurement of RTD

Sodium chloride was used as tracer, which was detected using a YSI3200 conductivity meter with YSI3445 flow-through cell (YSI, Ohio, USA) and a personal computer. The conductivity cell is a 15 mL annular glass tube with two small platinum–iridium electrodes. Water was used as test fluid, since its flow properties do not differ largely from milk (Tomasula and Kozempel, 2004). A low background concentration of NaCl (between 0.5 and 1.0 g/L) was kept to improve the strength of the conductivity signal. A small volume of 0.05 mL of saturated NaCl solution (~36 g/L) was injected through the silicon tubing at the desired process point using a 1.0 mL insulin syringe. The tested flow rates were 10, 15,

20, 25, 30 and 35 L/h. Data acquisition frequency varied between 1 and 5 s. The cell temperature was monitored using a digital thermometer with an exposed-junction type-K thermocouple (Instrutherm, São Paulo, Brazil).

Previously to the RTD runs, the conductivity of the NaCl solution was correlated to its concentration and temperature. For concentrations of 0.25, 0.50, 0.75, 1.00, 1.25, 1.50 and 1.75 g/L, electrical conductivity of the solution was measured for 35 temperatures between 17 and 31 °C (temperature step was 0.5 °C). Because of the small amount of tracer injected, the outlet concentration was under 1.75 g/L in the RTD runs. The temperature range was chosen because ambient temperature was approximately 25 °C. For each concentration, the conductivity was linearly correlated with temperature as $c = a_1 + a_2 \cdot T$. Parameters a_1 and a_2 were correlated with the concentration as $a_1 = a_3 \cdot C + a_4 \cdot C^2$ and $a_2 = a_5 \cdot C + a_6 \cdot C^2$. Consequently, the conductivity equation has four parameters as in Eq. (17). Parameters were estimated with Excel Solver for minimizing the sum of squared errors on the conductivity.

$$c = (a_3 \cdot C + a_4 \cdot C^2) + (a_5 \cdot C + a_6 \cdot C^2) \cdot T \quad (17)$$

This correlation was used to obtain the tracer concentration from the conductivity data. Subsequently, the E-curve was determined for each experimental run using Eq. (1). The integral in Eq. (1) was numerically evaluated by the trapezoidal method.

4.3. Determination of the detection system RTD

For each flow rate, experimental runs were conduced for the determination of the RTD of the detection system (conductivity sensor and data acquisition hardware). The mean residence time was obtained from Eq. (3) by trapezoidal method. Since the mean residence time is very short, at least six repetitions were performed for each flow rate.

The dispersion model in Eq. (5) and the tanks in series model in Eq. (7) were fitted to the data of each run for minimizing the sum of squared errors on E_θ in the dimensionless time domain. The mean Peclet numbers and mean numbers of tanks were correlated with the flow rate.

4.4. Determination of holding tubes RTD

Experimental runs were conducted in triplicate for each flow rate to obtain the RTD of holding tubes T1 and T2. The four RTD models presented in Section 2 were used to fit the experimental data in the time domain, minimizing Eq. (16). The procedure was according to Section 3.2 using a time step of 0.5 s. The adjusted model parameter and mean residence time were correlated with the flow rate.

5. Analysis of results and discussion

5.1. Conductivity curve

From the collected conductivity data, the four parameters of Eq. (17) were adjusted to minimize the sum of squared errors on c and the results are: $a_3 = 923.3$, $a_4 = -52.31$, $a_5 = 42.82$ and $a_6 = -2.424$ ($R^2 = 0.998$). Corresponding units for Eq. (17) are: c [μS/cm], T [°C] and C [g/L].

5.2. RTD of the detection system

The best fit of the detection system RTD was obtained with the axial dispersion model in Eq. (5). Fig. 5 shows an example of data fit for flow rate 20 L/h with nine experimental runs. The Peclet number was adjusted for each run and the mean value for 20 L/h ($Pe = 7.6$) was used for the model curve in Fig. 5.

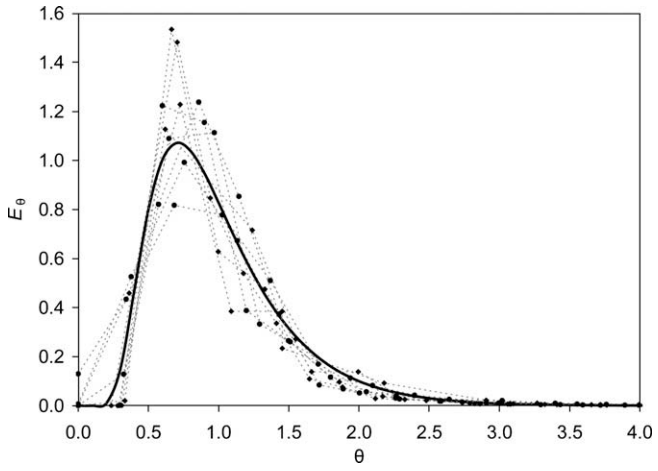

Fig. 5. Experimental runs for the determination of the RTD of the detection system at flow rate 20 L/h and adjusted dispersion model ($Pe = 7.6$).

Fig. 6 shows the flow rate dependence of mean residence time and Peclet number. Since it was not possible to detect a flow rate dependence on Pe, the mean value of 7.8 ± 1.8 was considered. The mean residence time was correlated with the flow rate

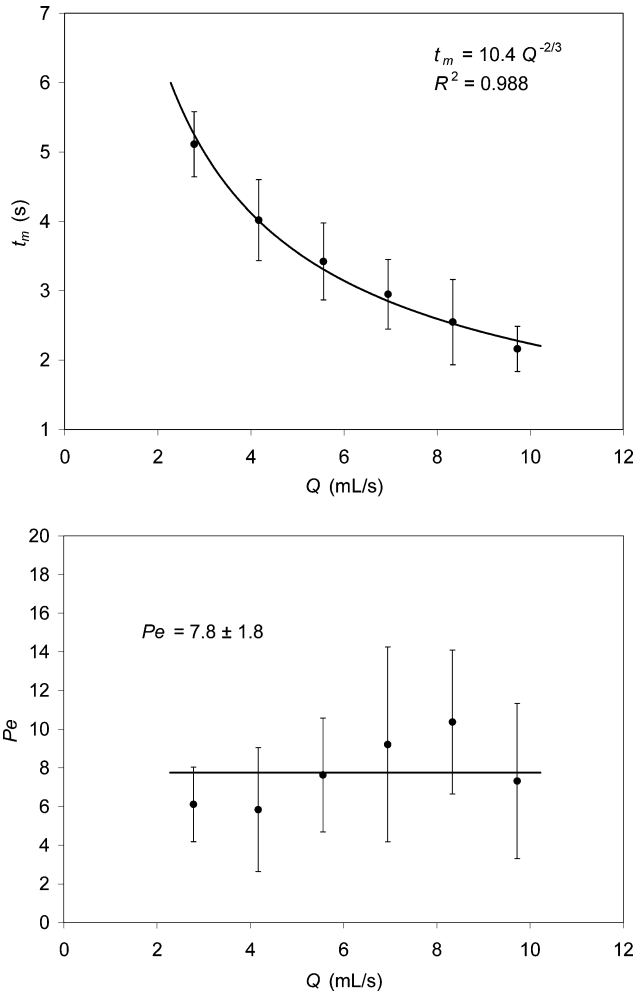

Fig. 6. Results of the detection system RTD and influence of flow rate.

through Eq. (18). Usually, a vessel would exhibit a correlation between t_m and Q in the form $t_m = V^A/Q$, where V^A is the active volume of the vessel. Eq. (18) does not have such form because the electrodes of the sensor are inside the studied vessel. The obtained results of t_m and Pe were used for the convolution of RTD functions, as described in Section 3.2

$$t_m(\mathrm{s}) = 10.4 \cdot Q\,(\mathrm{mL/s})^{-2/3} \tag{18}$$

5.3. RTD of the holding tubes

The RTD of the holding tubes was determined according to Section 4.4. Reynolds number for tube flow varied between 370 and 1290 for T1 and between 420 and 1490 for T2 ($Re = 4 \cdot Q \cdot \rho / \pi \cdot D_{in} \cdot \mu$). Fig. 7 brings examples of convolution and model adjustment with the generalized convection model, which was convoluted with the detection system E-curve for the same flow rate (dispersion model with $Pe = 7.8$ and t_m from Eq. (18)). The error between the convoluted curve and the experimental points was minimized in order to adjust the model parameter, θ_0, and the mean residence time, t_m.

In Fig. 7, the signal distortion caused by the detection system is clear. Fillaudeau et al. (2009) verified that the distortion of the inlet signal can be neglected if it does not exceed 1% of the mean residence time. In this work the mean residence time of the detection cell exceeds in more than 22% the mean residence time of T1 and 9% the mean residence time of T2. Thus, the convolution is required for the correct determination of the tube E-curve.

For both holding tubes, the generalized convection model provided a better fit, followed by the PFR + CSTR association model, as can be seen in Table 2. The dispersion and tanks in series models

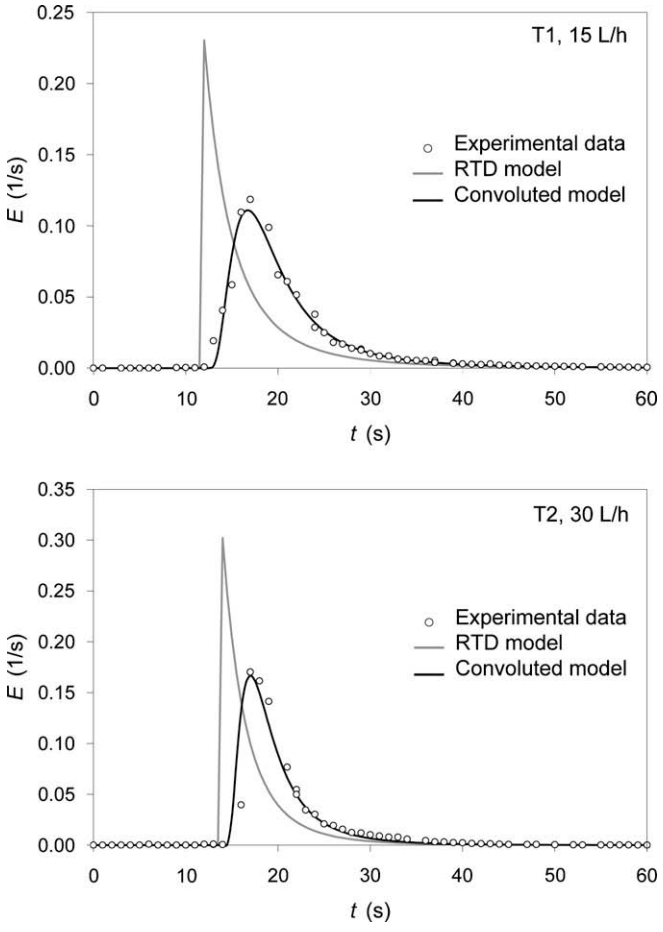

Fig. 7. Examples of adjustment of the generalized convection model using numerical convolution.

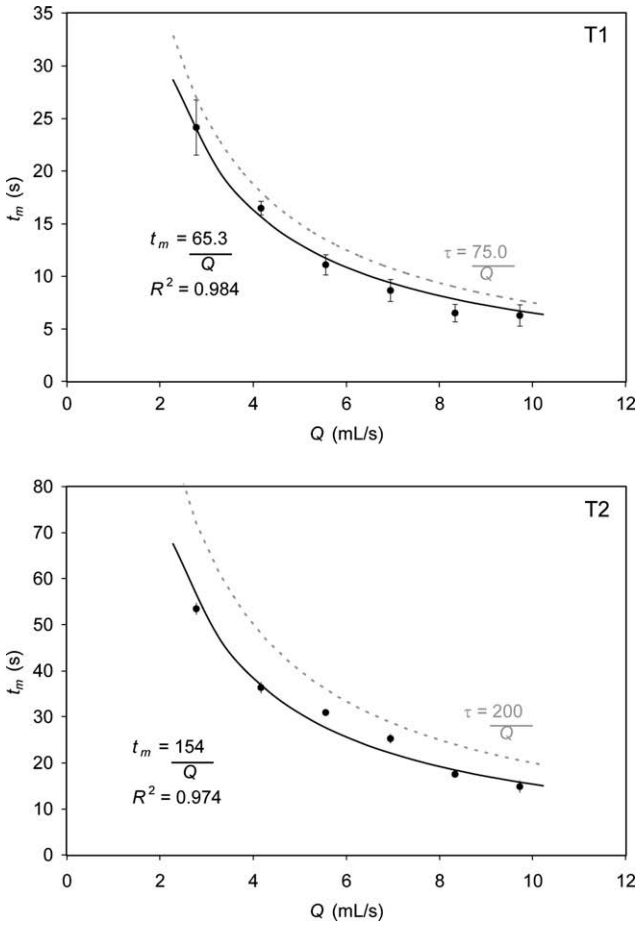

Fig. 8. Mean residence times for tubes T1 and T2 as affected by flow rate.

Table 2
Sum of squared errors on model fitting, $SSE \cdot 10^3$.

Tube	Model	Flow rate (L/h)					
		10	15	20	25	30	35
T1	Generalized convection	0.6 ± 0.2	3.0 ± 2.4	2.3 ± 1.6	2.9 ± 2.2	10.5 ± 1.8	3.4 ± 2.7
	PFR + CSTR combination	0.8 ± 0.4	3.5 ± 2.9	3.0 ± 1.4	2.7 ± 1.9	10.2 ± 1.2	3.0 ± 2.4
	Dispersion	3.4 ± 0.8	5.2 ± 1.9	5.9 ± 1.5	4.2 ± 2.1	8.8 ± 1.2	5.8 ± 8.3
	Extended tanks in series	4.2 ± 0.6	5.7 ± 1.9	6.5 ± 1.5	4.5 ± 2.2	13.0 ± 5.5	8.1 ± 2.9
T2	Generalized convection	0.8 ± 0.2	2.5 ± 1.0	2.4 ± 1.4	3.5 ± 1.7	3.5 ± 2.4	6.4 ± 3.8
	PFR + CSTR combination	1.7 ± 0.1	3.1 ± 1.2	3.3 ± 1.3	4.5 ± 2.5	8.7 ± 6.2	6.7 ± 3.5
	Dispersion	5.7 ± 0.3	10.5 ± 3.1	11.4 ± 1.7	14.3 ± 2.8	14.4 ± 7.7	16.8 ± 5.8
	Extended tanks in series	6.1 ± 0.3	10.9 ± 3.2	11.9 ± 1.6	15.1 ± 2.7	14.9 ± 7.8	17.5 ± 6.5

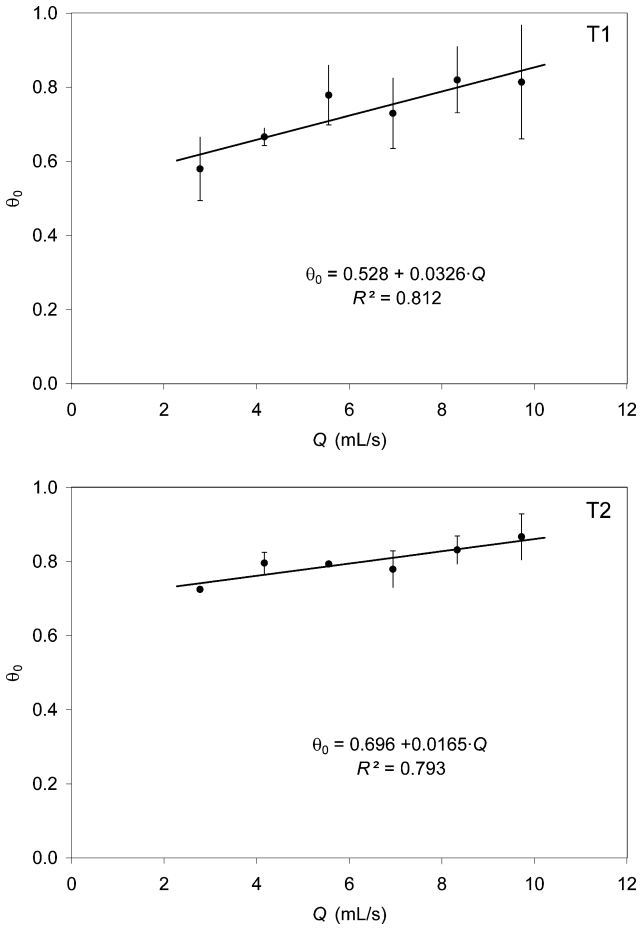

Fig. 9. Breakthrough time for tubes T1 and T2 as affected by flow rate.

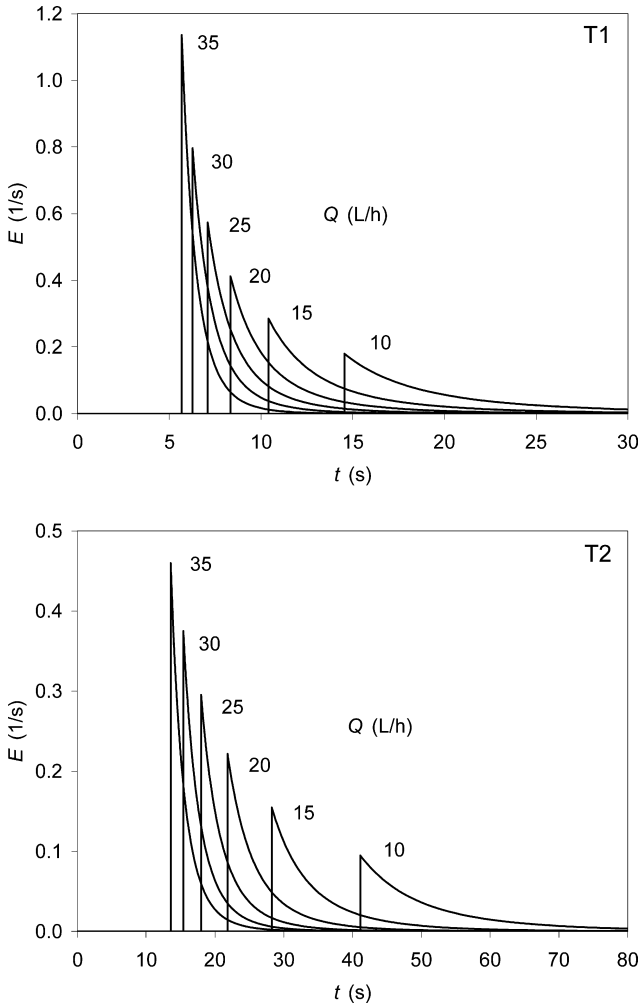

Fig. 10. Effect of flow rate on the RTD of holding tubes T1 and T2 using the adjusted generalized convection model.

failed to represent the tail seen in Fig. 7. Fig. 8 shows the adjusted mean residence time and the theoretical spatial time for tubes T1 and T2. The curve fit yields in active volumes of 65.3 and 154 mL for T1 and T2, respectively. These results indicate that T1 has a dead volume of 75.0 − 65.3 = 9.7 mL (13%) and T2 has a dead volume of 200 − 154 = 46 mL (23%). The dead volume consists of undesired stagnation and recirculation regions.

The influence of flow rate on model parameter θ_0 (breakthrough time) is shown in Fig. 9. Adjusted linear correlations for tube T1 and T2 are in Eqs. (19) and (20), respectively.

$$\theta_0 = 0.528 + 0.0326 \cdot Q(\mathrm{mL/s}) \quad (19)$$

$$\theta_0 = 0.696 + 0.0165 \cdot Q(\mathrm{mL/s}) \quad (20)$$

The theoretical breakthrough time for laminar flow in a straight tube is $\theta_0 = 0.5$. The values obtained in this work are above 0.5, which denotes a flatter velocity profile than the parabolic profile. For the limiting case of $\theta_0 = 1.0$, the Dirac delta is obtained (plug flow without dispersion). In the RTD studies of Ruthven (1971) and Trivedi and Vasudeva (1974) for helical tubes, breakthrough times between 0.586 and 0.658 were determined. The secondary flow circulation that is induced in curves reduces the spread of the residence time, which is consistent with a reduction of the breakthrough time in laminar flow, as can be seen in Fig. 1. Moreover, the peristaltic pump used in this work induces a weak pulsation on the flow rate and this oscillation can also make the velocity profile flatter.

Rao and Loncin (1974a) define the efficiency of a holding tube as the ratio between the minimum and the mean residence times. For the convection model, the minimum residence time is $t_{min} = \theta_0 \cdot t_m$; thus the efficiency is $\theta_0 \cdot 100\%$. The ideal cases of plug flow and laminar flow would present efficiencies of 100% and 50%, respectively. Generally, higher Reynolds numbers yields higher tube efficiencies (Torres and Oliveira, 1998b). Since the spread in the laminar flow RTD is reduced on curved tubes, the tube efficiency is higher than 50%, as verified in this work. However, the results indicate a considerable dead volume in the curved tubes.

The effect of the flow rate on the RTD of tubes T1 and T2 is illustrated in Fig. 10 using the adjusted generalized convection model. As expected, the E-curve has a larger spread for low flow rates and holding tube T1 has shorter residence times than T2.

6. Conclusions

It was possible to determine the RTD of the holding tubes using the proposed method that takes into account the non-ideal tracer detection. The method could be easily implemented on an electronic spreadsheet, which favors its applicability. This signal distortion was considerable since the mean residence time of the holding tubes was short for the tested flow rates. The generalized convection model provided the best fit, because it can model the tail on the tracer concentration curve that is caused by the velocity profile and the stagnant/recirculation regions. The generalized convection model proved to be useful for describing laminar flow in

curved tubes and the results suggested velocity profile flatter then the theoretical parabola. The obtained E-curves can be used for the evaluation of tube lethality on a given microorganism, enzyme or product attribute as described in the works of Rao and Loncin (1974b), Sancho and Rao (1992) and Lewis and Heppell (2000).

Acknowledgments

The authors would like to acknowledge financial support from FAPESP (The State of São Paulo Research Foundation) and to CAPES.

References

Burton, H., 1958. An analysis of the performance of an ultra-high-temperature milk sterilizing plant: I. Introduction and physical measurements. Journal of Dairy Research 25 (1), 75–84.

Chakrabandhu, K., Singh, R.K., 2006. Determination of food particle residence time distributions in coiled tube and straight tube with bends at high temperature using correlation analysis. Journal of Food Engineering 76 (2), 238–249.

Fillaudeau, L., Le-Nguyen, K., Andre, C., 2009. Influence of flow regime and thermal power on residence time distribution in tubular Joule effect heaters. Journal of Food Engineering 95 (3), 489–498.

Garcia-Serna, J., Garcia-Verdugo, E., Hyde, J.R., Fraga-Dubreuil, J., Yan, C., Poliakoff, M., Cocero, M.J., 2007. Modelling residence time distribution in chemical reactors: a novel generalised *n*-laminar model – application to supercritical CO_2 and subcritical water tubular reactors. Journal of Supercritical Fluids 41 (1), 82–91.

Gouvêa, M.T., Park, S.W., Giudici, R., 1990. Estimação de coeficientes de dispersão axial em leitos fixos. In: Anais do XVIII Encontro sobre escoamento em meios porosos, Nova Friburgo, October 23rd–25th.

Gut, J.A.W., Pinto, J.M., Gabas, A.L., Telis-Romero, J., 2005. Continuous pasteurization of egg yolk: thermophysical properties and process simulation. Journal of Food Process Engineering 28 (2), 181–203.

Heibel, A.K., Lebens, P.J.M., Middelhoff, J.W., Kapteijn, F., Moulijn, J., 2005. Liquid residence time distribution in the film flow monolith reactor. AIChE Journal 51 (1), 122–133.

Himmelblau, D.M., Bischoff, K.B., 1968. Process Analysis and Simulation: Deterministic Systems. Wiley, New York (Chapter 4).

Ibarrola, J.J., Sandoval, J.M., García-Sanz, M., Pinzolas, M., 2002. Predictive control of a high temperature–short time pasteurization process. Control Engineering Practice 10 (7), 713–725.

Levenspiel, O., 1999. Chemical Reaction Engineering, third ed. John Wiley & Sons, New York.

Levenspiel, O., 1989. The Chemical Reactor Omnibook. OSU, Corvallis.

Levenspiel, O., Bischoff, K.B., 1963. Patterns of flow in chemical process vessels. In: Drew, T.B., Hoopes, J.W., Vermeulen, T. (Eds.), Advances in Chemical Engineering, vol. 4. Academic Press, New York.

Levien, K.L., Levenspiel, O., 1999. Optimal product distribution from laminar flow reactors: Newtonian and other power-law fluids. Chemical Engineering Science 54 (13–14), 2453–2458.

Lewis, M., Heppell, N., 2000. Continuous Thermal Processing of Foods: Pasteurization and UHT Sterilization. Aspen Publishers, Gaithersburg.

Martin, A.D., 2000. Interpretation of residence time distribution data. Chemical Engineering Science 55 (23), 5907–5917.

Mills, P.L., Dudukovic, M.P., 1989. Convolution and deconvolution of nonideal tracer response data with application to 3-phase packed-beds. Computers and Chemical Engineering 13 (8), 881–898.

Nauman, E.B., 1977. The residence time distribution for laminar-flow in helically coiled tubes. Chemical Engineering Science 32 (3), 287–293.

Rangaiah, G.P., Krishnaswamy, P.R., 1990. Application of time domain curve-fitting to parameter-estimation in RTD models. Journal of Chemical Engineering of Japan 23 (2), 124–130.

Rao, M.A., Loncin, M., 1974a. Residence time distribution and its role in continuous pasteurization (Part I). Lebensmittel-Wissenschaft and Technologie 7, 5–13.

Rao, M.A., Loncin, M., 1974b. Residence time distribution and its role in continuous pasteurization (Part II). Lebensmittel-Wissenschaft and Technologie 7, 14–17.

Ruthven, D.M., 1971. The residence time distribution for ideal laminar flow in a helical tube. Chemical Engineering Science 26, 1113–1121.

Sancho, M.F., Rao, M.A., 1992. Residence time distribution in a holding tube. Journal of Food Engineering 15 (1), 1–19.

Tomasula, P.M., Kozempel, M.F., 2004. Flow characteristics of a pilot-scale high temperature, short time pasteurizer. Journal of Dairy Science 87 (9), 2761–2768.

Torres, A.P., Oliveira, F.A.R., 1998b. Residence time distribution of liquids in a continuous tubular thermal processing system – Part II: relating hold tube efficiency to processing conditions. Journal of Food Engineering 35 (2), 165–175.

Torres, A.P., Oliveira, F.A.R., 1998a. Residence time distribution studies in continuous thermal processing of liquid foods: a review. Journal of Food Engineering 36 (1), 1–30.

Torres, A.P., Oliveira, F.A.R., Fortuna, S.P., 1998. Residence time distribution of liquids in a continuous tubular thermal processing system – Part I: relating RTD to processing conditions. Journal of Food Engineering 35 (2), 147–163.

Trivedi, R.N., Vasudeva, K., 1974. RTD for diffusion free laminar-flow in helical coils. Chemical Engineering Science 29 (12), 2291–2295.